# Application of structured illumination for multiple scattering suppression in planar laser imaging of dense sprays

**Edouard Berrocal[1]*, Elias Kristensson[1], Mattias Richter[1], Mark Linne [1, 2] and Marcus Aldén[1]**

[1] *Department of Combustion Physics, Lund Institute of Technology, Box 118, Lund 221 00, Sweden*
[2]*Sandia National Laboratories, P.O. Box 969, Livermore, California 94551, USA*
[*]*Corresponding author: edouard.berrocal@forbrf.lth.se*

**Abstract:** A novel approach to reduce the multiple light scattering contribution in planar laser images of atomizing sprays is reported. This new technique, named **S**tructured **L**aser **I**llumination **P**lanar **I**maging (**SLIPI**), has been demonstrated in the dense region of a hollow-cone water spray generated in ambient air at 50 bars injection pressure. The idea is based on using an incident laser sheet which is spatially modulated along the vertical direction. By properly shifting the spatial phase of the modulation and using post-processing of the successive recorded images, the blurring effects from multiple light scattering can be mitigated. Since hollow-cone sprays have a known inner structure in the central region, the efficiency of the method could be evaluated. We demonstrate, for the case of averaged images, that an unwanted contribution of 44% of the detected light intensity can be removed. The suppression of this diffuse light enables an increase from 55% to 80% in image contrast. Such an improvement allows a more accurate description of the near-field region and of the spray interior. The possibility of extracting instantaneous flow motion is also shown, here, for a dilute flow of water droplets. These results indicate promising applications of the technique to denser two-phase flows such as air-blast atomizer and diesel sprays.



**OCIS codes:** (290.4210) Multiple scattering; (110.0113) Imaging through turbid media; (280.2490) Flow diagnostics; (100.2980) Image enhancement

## References and links

1. R. J. Adrian, "Twenty years of particle image Velocimetry," Exp. Fluids **39**, 159-69 (2005).
2. H.-G. Maas, A. Grün, and D. Papantoniou, "Particle Tracking in three dimensional turbulent flows - Part I: Photogrammetric determination of particle coordinates," Exp. Fluids. **15**, 133-146 (1993).
3. L. A. Melton and J. F. Verdieck, "Vapor/liquid visualization for fuel sprays," in *Proceedings of the 20th International Symposium on Combustion* (The Combustion Institute, Pittsburgh, Pa., 1984), pp. 1283–1290.
4. A. Serpenguzel, S. Kucuksenel, and R. K. Chang, "Microdroplet identification and size measurement in sprays with lasing images," Opt. Express **10**, 1118-1132 (2002).
5. R. Domann and Y. Hardalupas, "Quantitative measurement of planar droplet Sauter mean diameter in sprays using planar droplet sizing," Part. Part. Syst. Charact. **20**, 209-218 (2003).
6. P. LeGal, N. Farrugia, and D. A. Greenhalgh, "Laser sheet dropsizing of dense sprays," Opt. Laser Technol. **31**, 75–83 (1999).
7. E. Berrocal, Multiple scattering of light in optical diagnostics of dense sprays and other complex turbid media (PhD Thesis, Cranfield University, 2006).
8. E. Berrocal, I. Meglinski, and M. Jermy, "New model for light propagation in highly inhomogeneous polydisperse turbid media with applications in spray diagnostics," Opt. Express **13**, 9181-9195 (2005).
9. D. Stepowski, O. Werquin, C. Roze, and T. Girasole, "Account for extinction and multiple scattering in planar droplet sizing of dense sprays," in *13th International Symposium on Applications of Laser Techniques to Fluid Mechanics* (Lisbon, 2006), paper 1061.

#100992 - $15.00 USD Received 2 Sep 2008; revised 9 Oct 2008; accepted 15 Oct 2008; published 20 Oct 2008

10. C. T. Brown, V. G. McDonell, and D. G. Talley, "Accounting for laser extinction, signal attenuation, and secondary emission while performing optical patternation in a single plane," ILASS Americas 15th Ann. Conf. on Liquid Atomization and Spray Systems (Madison, WI: ILASS-Americas 2002).
11. H. M. Hertz and M. Aldén, "Calibration of imaging laser-induced fluorescence measurements in highly absorbing flames," Appl. Phys. B **42**, 97–102 (1987).
12. R. Abu-Gharbieh, J. L. Persson, M. Forsth, A. Rosen, A. Karlstrom, and T. Gustavsson, "Compensation method for attenuated planar laser images of optically dense sprays," Appl. Opt. **39**, 1260-1267 (2000).
13. D. G. Talley, J. F. Verdieck, S. W. Lee, V. G. McDonnell, and G. S. Samuelsen, "Accounting for laser sheet extinction in applying PLLIF to sprays," paper AIAA-96–0469, presented at the Thirty-Fourth Aerospace Sciences Meeting, Reno, Nev., 15–18 Jan. 1996 (American Institute of Aeronautics and Astronautics, New York, 1996).
14. V. Sick and B. Stojkovic, "Attenuation effects on imaging diagnostics in hollow-cone sprays," Appl. Opt. **40**, 2435-2442 (2001).
15. H. Koh, J. Jeon, D. Kim, Y. Yoon, and J-Y Koo, "Analysis of signal attenuation for quantification of planar imaging technique," Meas. Sci. Technol. **14** 1829-39 (2003).
16. M. A. A. Neil, R. Juskaitis, and T. Wilson, "Method of obtaining optical sectioning by using structured light in a conventional microscope," Opt. Lett. **22**, 1905-1907 (1997).
17. T. Breuninger, K. Greger, and E. H. K. Stelzer, "Lateral modulation boosts image quality in single plane illumination fluorescence microscopy," Opt. Lett. **32**, 1938-1940 (2007).
18. S. E. D. Webb, Y. Gu, S. Lévêque-Fort, J. Siegel, M. J. Cole, K. Dowling, R. Jones, P. M. W. French, M. A. A. Neil, R. Juskaitis, L. O. D. Sucharov, T. Wilson, and M. J. Lever, "A wide-field time-domain fluorescence lifetime imaging microscope with optical sectioning", Rev. Sci. Instrum. **73**, 1898-1907 (2002).
19. B. P. Husted, Experimental measurements of water mist systems and implications for modelling in CFD (PhD Thesis, Lund University, 2007).
20. E. Kristensson, E. Berrocal, M. Richter, S-G. Pettersson, and M. Aldén, "High-speed structured planar laser illumination for contrast improvement of two phase flow images," Accepted for publication in Opt. Lett.

## 1. Introduction

Due to their non-intrusive nature, laser imaging techniques are largely used for the study of scattering media and have numerous applications from combustion engineering to medical research. Depending on the source/detector arrangement, imaging can be performed using the back, forward or side scattering detection. One of the most popular side scattering detection methods for flow visualization is planar laser imaging. This approach is widely employed in the field of spray diagnostics in order to provide qualitative and quantitative two-dimensional information on spray structure. Depending on the physical quantities measured, a number of planar laser imaging techniques have been developed during the past three decades. The most common ones are Particle Image Velocimetry [1], Particle Tracking Velocimetry [2] , Planar Laser Induce Fluorescence [3], droplet lasing [4] and Planar Drop Sizing [5] also known as Laser Sheet Dropsizing [6]. Although these techniques use different properties of light scattering and instrumental approaches, they are all based on the single scattering approximation; assuming that the detected photons have experienced only one scattering event prior to arrival at the detector. This assumption remains valid when the number density of particles is low and when the total photon path length within the probed medium is short. However, within optically dense media (e.g. the near-field spray region) a large amount of photons are scattered more than once and the single scattering assumption is no longer valid. In this case, the multiple light scattering blurs and attenuates the recorded images, introducing significant uncertainties in the detected optical signal [7]. This contribution from multiply scattered photons is particularly important in planar imaging, due to the use of both a relatively wide source of light and a large detection acceptance angle of the collection optics. It has been calculated using a numerical Monte Carlo approach, that only 24% of the total number of detected photons are singly scattered for planar Mie imaging of a typical hollow-cone spray [7-8]. Other Monte Carlo calculations [9] have been tested for an air-blast atomizer with relative high transmission (71%), showing that multiple scattering effects were relevant in the Mie signal but were, on the contrary, almost non-existent in the LIF signal. Such results demonstrate that errors introduced by the multiple light scattering cannot be simply cancelled from the ratio LIF/Mie and requires much more advanced corrections. In addition to multiple

#100992 - $15.00 USD Received 2 Sep 2008; revised 9 Oct 2008; accepted 15 Oct 2008; published 20 Oct 2008

scattering issues (also known in the literature as *secondary emission* [10]) two other typical sources of error occur when probing the dense spray region. The first one is due to the laser intensity reduction along its direction of propagation, referred as *laser light extinction* and the second one concerns the reduction of the signal between the laser sheet and the detector, referred as *signal attenuation*. Various procedures have been employed in order to correct and compensate errors introduced by *laser light extinction*: One solution consists in post-processing the data using numerical algorithms based on the iterative inversion of the Beer-Lambert law [11-12]. Another solution is to experimentally use bidirectional illumination by means of sequential excitations from counter-propagating laser sheets. Such techniques have been applied for both Planar Liquid Laser Induce Fluorescence and planar Mie imaging [13-15]. In addition to these corrections, other methods have been tested to account for *signal attenuation* [10, 15]. However, due to the complexity in predicting and understanding effects introduced by multiple scattering, no experimental technique has been proposed, so far, for the correction of the *secondary emission*.

In this study we investigate the possibility to suppress this multiply scattered light from the detected image by using Structured Laser Illumination Planar Imaging (SLIPI). This technique is inspired by Structured Illumination Microscopy (SIM) [16] but is implemented here in a planar laser imaging configuration similar to the work first published by Breuninger *et al*. known as Single Plane Illumination Microscopy – Structured Illumination (SPIM-SI) [17]. Unlike to Breuninger's application, which concerns the study of static solid objects at microscopic scale, we are imaging dynamic liquid structures from high-velocity two-phase flows at a submillimetre scale. Furthermore, we detect the elastic Mie scattering signal instead of an inelastic fluorescence signal. In the work reported here, the probed medium is a hollow-cone water spray operating in the atomization regime. Particular attention is given to the dense spray region where conventional methods are hampered by errors due to multiple scattering. A quantitative estimation of the image improvement is performed based upon direct comparison between the conventional and the SLIPI image. In parallel to these measurements, another droplet flow, generated by a nebuliser, has been probed. This flow is more dilute and slower than the hollow-cone spray and it has been employed in order to demonstrate the capability of the technique to freeze the motion of the flow. The study of the hollow cone spray was based on recording an average of 50 single SLIPI images; whereas, a "single shot" SLIPI image was considered for the case of the nebulizer.

This article is structured as follows: In the first section the principle of the technique is explained using some theoretical considerations. The second section describes the experimental set-up. The third section highlights the main results, for both the hollow-cone spray and the nebulizer. Finally, a discussion regarding the efficiency of the method with its future application is provided.

## 2. The structured illumination method

Structured illumination is based on spatial intensity modulation of the input light. Such a modulation can be created by projecting the image of a grating onto the sample of interest. In microscopy, structured illumination can be used to remove out-of-focus photons, which may cause blurring effects on the resulting image. Similar unwanted effects can be observed in planar laser measurements caused by the multiple light scattering. By using intensity modulated light, it is possible to suppress this unwanted interference during image post-processing. Here, the main idea is that photons which have experienced several scattering events within the sample will lose modulation information on the way to the imaging system, while singly scattered photons will not. Illuminating a sinusoidal grating and focusing the image into the measurement region results in a normalized amplitude fringe pattern $s(x,y)$ of the functional form

$$s(x,y) = 1 + m \,.\, \cos\left(2\pi\, v\, y + \Phi_0\right) \tag{1}$$

#100992 - $15.00 USD Received 2 Sep 2008; revised 9 Oct 2008; accepted 15 Oct 2008; published 20 Oct 2008

where $m$ denotes the modulation depth, $v$ is the spatial frequency, $\Phi_0$ is an arbitrary spatial phase while $x$ and $y$ are the coordinate axes. Such an illumination leads to an image $I(x,y)$ [17] according to

$$I(x,y) = I_C + I_S \cdot \cos(2\pi v y + \Phi_0) \tag{2}$$

This collected light $I(x,y)$ can be divided into two different images, denoted $I_C$ and $I_S$. The first image $I_C$ contains both single and multiple light scattering, and is referred to as the *conventional* image later in the text. This image describes how the captured image would look if there were no modulation. The second image $I_S$ contains mainly singly scattered photons and corresponds to the SLIPI image. The cosine term describes the superimposed fringe pattern, which must be removed in order to obtain the SLIPI image $I_S$. This can be achieved by recording three images, $I_1$, $I_2$ and $I_3$, with the relative spatial phases $\Phi_0 = 0$, $2\pi/3$ and $4\pi/3$ as shown in Fig. 1(d) and Fig. 2. When changing the phase, the intensity modulation is moved along the vertical axis and a change of $2\pi/3$ will shift the modulation a third of a period. However, the multiple light scattering, which is superimposed on the intensity modulation, is unaffected by this shift. By calculating the pair-wise difference between the three recorded images, most of the multiply scattered light is removed. This is described by the following equation [17]:

$$I_S = \frac{\sqrt{2}}{3} \cdot \left[ (I_1 - I_2)^2 + (I_1 - I_3)^2 + (I_2 - I_3)^2 \right]^{1/2} \tag{3}$$

$$\text{and} \quad I_C = \frac{I_1 + I_2 + I_3}{3} \tag{4}$$

As mentioned above, if an object is illuminated with a modulated laser sheet, the vertical cross-section at a given distance $x = x'$, will result in a signal $I(x',y)$. An illustration of such a signal is given in Fig. 1(c). The modulated and the non-modulated components of this signal are shown in Fig. 1(b) and (a) respectively.

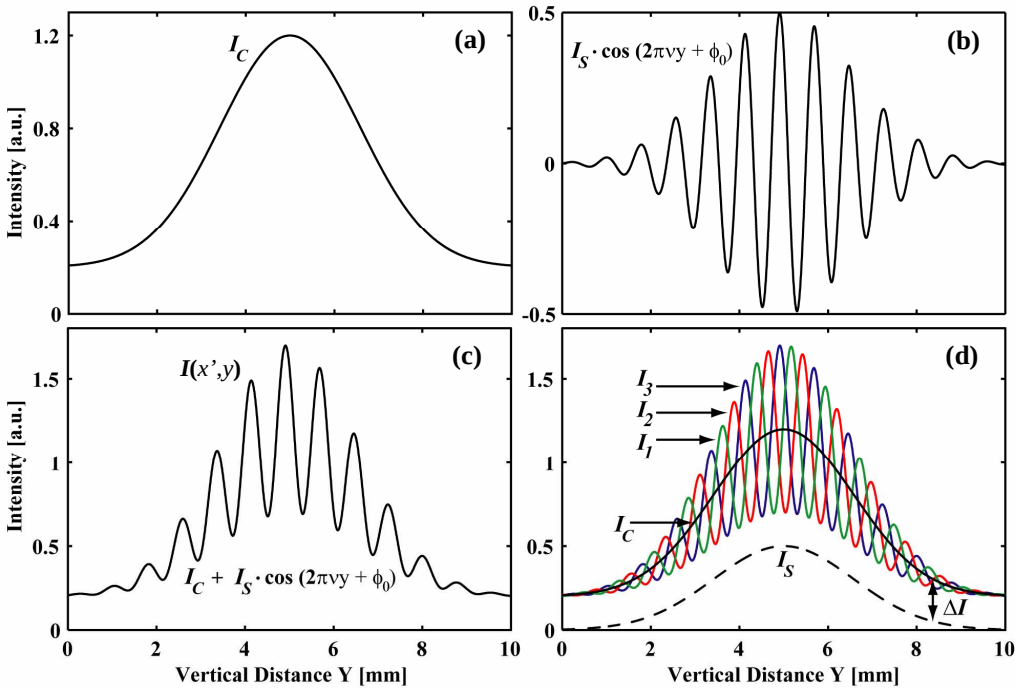


Fig. 1. Illustration of the conventional (a) and modulated components (b) with the resultant signal $I(x',y)$ in (c) for a given distance $x = x'$. Using three signals $I(x',y)$ each shifted one third of a period relative to each other, the SLIPI signal $I_S$ can be extracted as seen in (d).

#100992 - $15.00 USD Received 2 Sep 2008; revised 9 Oct 2008; accepted 15 Oct 2008; published 20 Oct 2008

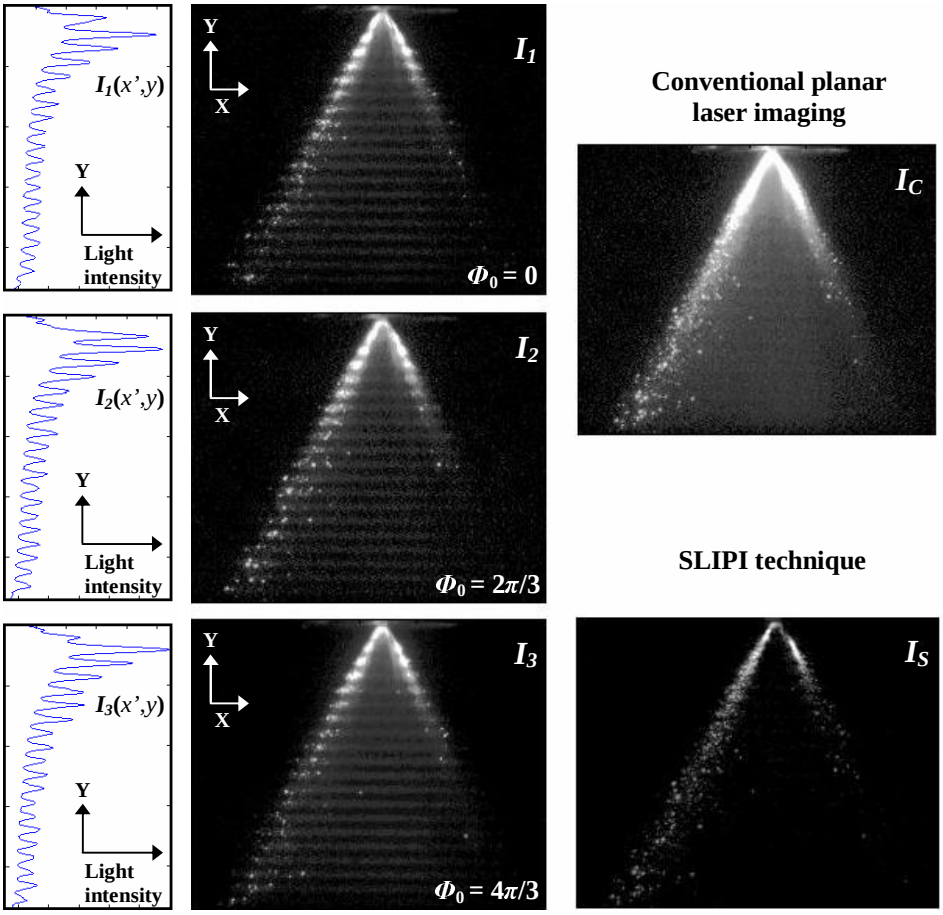


Fig. 2. Illustration of the SLIPI technique: 3 successive images are taken by illuminating different parts of the spray after shifting the spatial modulation one third of a period. When summing up the images, the conventional $I_C$ is obtained, whereas, when extracting the absolute value of the differences between the images, a new image $I_S$ is formed without most of the multiple light scattering. The modulated signal $I(x',y)$ is given for each image on the left side of the figure, at a given distance $x = x'$.

Thus, both the conventional and the SLIPI image can be extracted from three spatially modulated images. Photons scattered more than once give rise to a global blurring effect in each of the three successive images $I_1$, $I_2$ and $I_3$. On the contrary, the singly scattered photons which carry the structural information will differ from image to image due to the induced phase shift. The global blurring can then be removed by implementing Eq. (3). This process, which is illustrated in Fig. 2, operates as a directional filter and extracts most of the singly scattered photons, significantly improving the image contrast.

Note that for an increase of the optical depth, the modulation depth $m$ decreases since fewer photons are directly scattered into the camera. At large optical depths almost all light is multiply scattered reducing the modulation depth of $I_1$, $I_2$ and $I_3$ to near zero, together with the intensity of the SLIPI image. In other words, if no modulation is apparent within the three recorded images, the information is lost and the SLIPI image cannot be extracted. Such effects occur at very high optical density and present one of the main limiting factors of the technique.

#100992 - $15.00 USD Received 2 Sep 2008; revised 9 Oct 2008; accepted 15 Oct 2008; published 20 Oct 2008

## 3. Experimental set-up

In the work described here, both spray flow-fields were illuminated by a coherent laser source at a wavelength of 532 nm. The laser sheet was formed using a negative cylindrical lens combined with a positive spherical lens, and spaced a distance equal to the sum of their focal lengths. The resulting laser sheet dimension in the middle of the spray was ~1 mm wide and 25 mm high. The images $I_1$, $I_2$ and $I_3$ were recorded from three successive laser pulses (10 ns time-width), which were generated from two Nd:YAG lasers; one running in a single pulsed mode, while the second one was running in a double pulsed mode. All beams were then recombined to spatially overlap. The grid pattern was shifted a third of a period between the three pulses by using a rotating plane-parallel quartz plate. The individual beams entered the glass plate at different angles shifting the beams and the modulation pattern vertically. The spatial frequency of the grid was 10 line pair /mm producing a spatial modulation period of ~1 mm after magnification. By appropriately positioning the lenses and the grating, an image of the grid pattern was obtained in the centre of the spray and imaged at 90º.

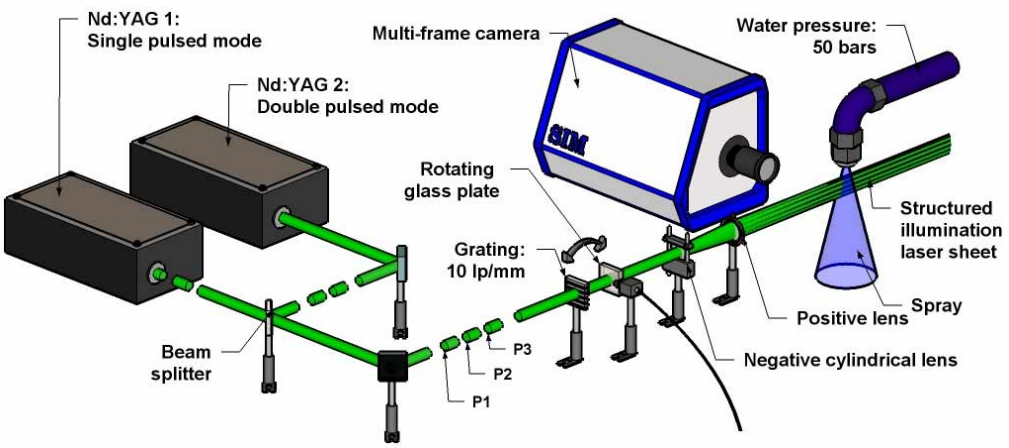


Fig. 3. Illustration of the experimental set-up: The time separation $\Delta t$ between each laser pulses (P1, P2 and P3) was 55 $\mu$s. By applying the appropriate rotation frequency, the rotating plate moved the modulated structure vertically one third of a period from pulse to pulse.

The images were acquired with a framing camera, using three 12-bit intensified CCDs each with an array of 960 X 1280 pixels. Each CCD array imaged an individual pulse (P1, P2 or P3) and each pixel corresponded to an imaged area of 25 $\mu$m square. The time separation $\Delta t$ between pulses is governed by both the rotation speed of the quartz plate and the spatial frequency of the grating. Note that $\Delta t$ is neither limited by the laser system nor by the multi-frame camera and it equaled 55 $\mu$s between each pulse. For this delay, a fluid displacement from pixel to pixel can be noticed only if the velocity motion is larger than 25 cm/s. Due to the high flow rate of the hollow-cone spray, $I_S$ and $I_C$ were extracted from averaged images (over 50 shots). However, "single shot" SLIPI images could be recorded for the case of the much slower nebulizer.

The nozzle employed in the experiment was a *Danfoss* 1910 pressure-swirl nozzle type, producing a hollow-cone with nominal 56º cone angle. This type of nozzle creates a water mist commonly employed to extinguish fires. Here, water was sprayed at an injection pressure of 50 bars into an atmospheric pressure optical chamber. At 3 mm below the nozzle tip, 26.5% light transmission was measured, corresponding to an optical depth of 1.33. Previous PDA measurements have indicated an average droplet size of ~20 $\mu$m in diameter within this spray [19].

#100992 - $15.00 USD Received 2 Sep 2008; revised 9 Oct 2008; accepted 15 Oct 2008; published 20 Oct 2008

## 4. Results and discussion

### *4.1 Application to a hollow-cone spray*

Results from two different experimental configurations are presented in this subsection. In the first configuration, measurements were performed along the central axis of the spray whereas in the second one the planar illumination was ~5 mm off-axis, behind the nozzle centre.

Figure 4 shows the central illumination where (a) corresponds to the conventional images, and the SLIPI image is shown in (b). The laser sheet entered the spray from the left side. A magnified area indicated with the dashed box (11 mm X 5 mm) is presented in Fig. 4(c) and (d). This area is situated 2.5 mm from the nozzle tip and corresponds to the dense region of the spray. In order to quantify the effectiveness of the method, the scattered light intensity profile along the horizontal axis has been plotted for 4 different positions (indicated by the arrows in Fig. 4(c)) below the nozzle tip. These intensity profiles are normalized with the maximum value of the conventional magnified image.

In the middle of the spray, no droplets were generated from the pressure swirl nozzle creating an inner conical structure. The intensity of the signal recorded from this region corresponds only to the light scattered from very small drops which have been transported in the central region due to vortical air flow. This intensity should, in principle, be much lower than the intensity originating from the side of the spray where the liquid volume fraction is much higher. However, due to multiple scattering, a large amount of photons falsely appear as though originating from the centre of the spray, as observed in Fig. 4(a) and (c). From the intensity profiles of the conventional image, it is seen that the light intensity along the centerline equals 0.11 at Y = 2.5 mm and is gradually reduced to 0.05 at Y = 6.3 mm, when moving away from the near-field region. This intensity decay is not observed in the SLIPI profiles where a constant value of only ~ 0.01 is measured at each position.

These profiles also highlight the two peaks of intensity arising from the liquid breakup regions. The first maximum corresponds to the side where the laser beam enters the spray. In this case, only small effects are introduced by *laser light extinction* and the contribution of singly scattered photons is large. On the contrary, the second maximum, which corresponds to the light scattered from the other side of the spray, is strongly affected by *laser light extinction*. This explains the reduction of the light intensity between the first and the second peak observed in Fig. 4(e), (f), (g) and (h), for both the conventional and the SLIPI signal. However, the contribution from multiple scattering is higher in the second peak of $I_C$, compared to the first one, due to the longer photon path-length within the spray. Therefore, if the intensity contribution from the *secondary emission* is removed, a higher ratio between the two peaks should be obtained. The calculations of the ratio $I_{max\ 1}$ / $I_{max\ 2}$ indicated in Table.1 show higher values for SLIPI than for the conventional case. These results demonstrate that the light intensity from *secondary emission* is removed by SLIPI, also in the densest scattering regions of the spray. Thus, for the conventional image, the difference of magnitude between the intensity peaks is due to *laser light extinction*, *signal attenuation* and *secondary emission* (assuming the spray to be symmetrical); whereas, for the SLIPI image, this difference is only governed by *laser light extinction* and *signal attenuation*.

From Fig. 4(e), (f) and (g) it is seen that the maximum light intensity difference $\Delta I$ between the conventional and the SLIPI profile is located just after the first intensity peak. At this location, the SLIPI profile decreases sharply to its minimum value, whereas the conventional profile presents a smoother decay. Also when suppressing the multiple light scattering, variations of intensity are more apparent, increasing the sharpness of the image. An estimation of the image improvement is performed based on the calculation of the Michelson contrast $C_1$ and $C_2$ for both the first peak and the second peak, such as

$$C_1 = \frac{I_{\max 1} - I_{\min}}{I_{\max 1} + I_{\min}} \qquad \text{and} \qquad C_2 = \frac{I_{\max 2} - I_{\min}}{I_{\max 2} + I_{\min}} \tag{5}$$

where, $I_{max1}$, $I_{max2}$ and $I_{min}$ are the respective maximum and minimum light intensity values indicated in Fig. 4(e).

#100992 - $15.00 USD Received 2 Sep 2008; revised 9 Oct 2008; accepted 15 Oct 2008; published 20 Oct 2008

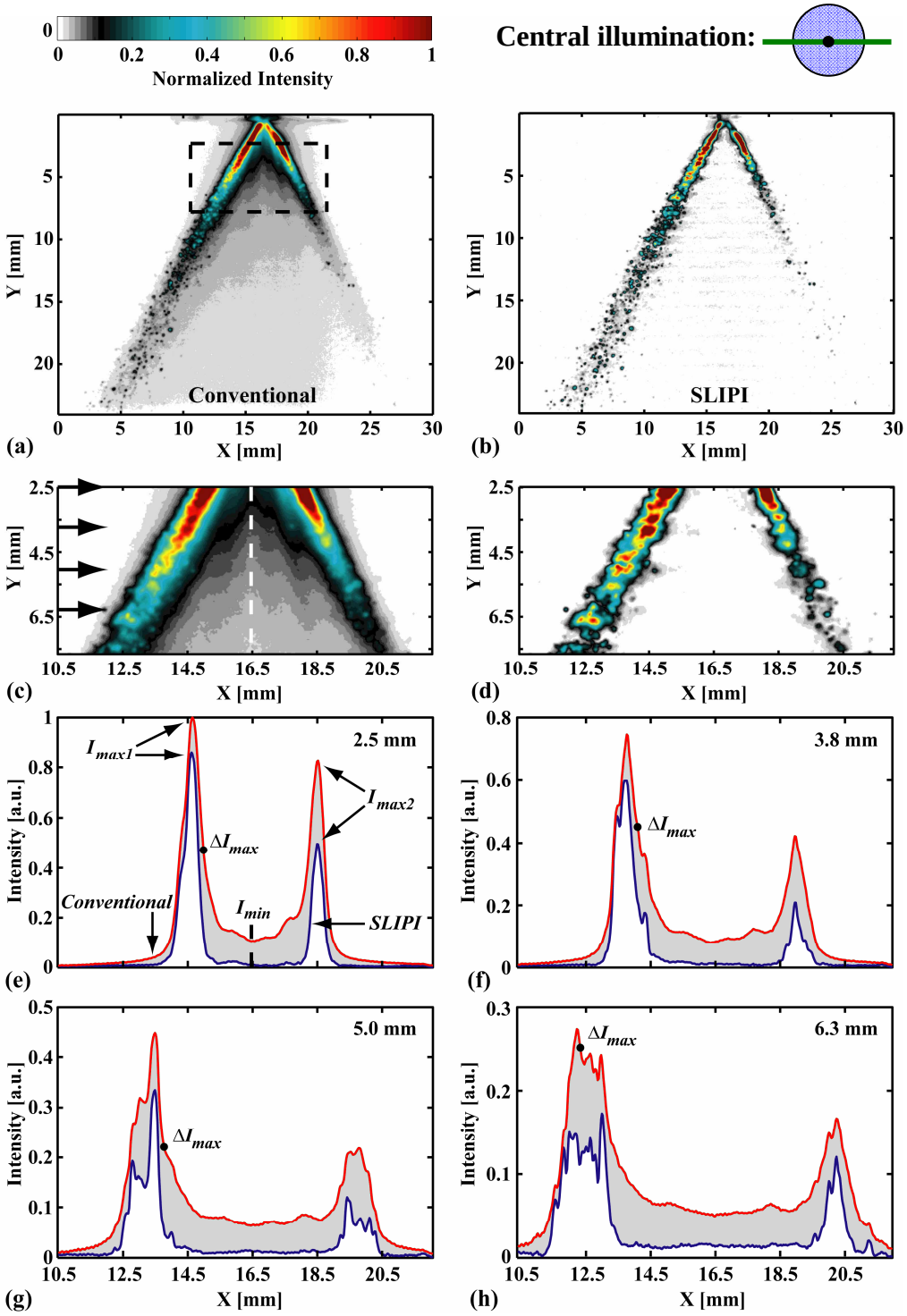


Fig. 4. Comparison between the conventional planar Mie imaging and SLIPI for the central illumination. Each image corresponds to an average of 50 triple images. A magnified area indicated by the dashed lines in (a) is illustrated for the conventional and the SLIPI image in (c) and (d) respectively. The intensity profile along the horizontal direction is given at four vertical positions indicated by the arrows in (c).

#100992 - $15.00 USD Received 2 Sep 2008; revised 9 Oct 2008; accepted 15 Oct 2008; published 20 Oct 2008

As seen in Table.1 $C_1$ and $C_2$ have been evaluated at each vertical position. At each of these positions, it is seen that $C_1$ is higher than $C_2$, pointing out the difference in contrast between the two sides of the spray image.

At Y = 2.5 mm, the multiple scattering contribution in the centre of the spray relative to the first peak equals 11% in $I_C$ and 1.5% in $I_S$. This leads to an increase in contrast from 80% to 97% between the two images. At Y = 5 mm, this amount of multiply scattered light detected in the conventional image equals 14% of the first peak and 29% of the second peak. However, for the SLIPI image these values are reduced to 3.9% and 11%, respectively. From these results, the contrast increase from 75% to 92% for the first peak and from 55% to 80% for the second peak. These results, which are summarized in Table1, demonstrate how the image contrast can be improved by means of SLIPI.

Table 1. Characteristics of the light intensity profiles given in Fig.4 (e), (f), (g) and (h). An estimation of the imagecontrast is provided at different locations within the spray for both the conventional and the SLIPI image.

| | **Conventional** | | | | **SLIPI** | | | |
|---|---|---|---|---|---|---|---|---|
| **Vertical position [mm]** | **2.5** | **3.8** | **5.0** | **6.3** | **2.5** | **3.8** | **5.0** | **6.3** |
| $I_{max1}$ / $I_{max2}$ | 1.22 | 1.79 | 2.05 | 1.59 | 1.72 | 2.86 | 2.75 | 1.42 |
| $I_{min}$ / $I_{max1}$ [%] | 11 | 11 | 14 | 19 | 1.5 | 2.1 | 3.9 | 9 |
| $I_{min}$ / $I_{max2}$ [%] | 13 | 19 | 29 | 30 | 2.5 | 6.1 | 11 | 12.9 |
| $C_1$ [%] | 80 | 80 | 75 | 69 | 97 | 96 | 92 | 83 |
| $C_2$ [%] | 77 | 68 | 55 | 53 | 95 | 88 | 80 | 77 |

| | | | | |
|---|---|---|---|---|
| $C_{1\ SLIPI}$ / $C_{1\ conventional}$ | 1.21 | 1.20 | 1.23 | 1.20 |
| $C_{2\ SLIPI}$ / $C_{2\ conventional}$ | 1.23 | 1.29 | 1.45 | 1.45 |

The off-axis illumination is presented Fig. 5 where (a) corresponds to the conventional image and (b) is the SLIPI image. In this configuration, multiple scattering should, on one hand, increase due to the longer photon mean-path within the spray but should, on the other hand, decrease since the densest region is no longer illuminated. Similar to the previous case, the laser sheet enters the spray on the left side and a magnified area (defined by the dashed box - 11 mm X 5 mm) is investigated in Fig. 5(c) and (d). As the laser sheet is located ~5 mm behind the nozzle tip, almost no optical signal should be detected from the near-field spray region as the liquid volume fraction tends to zero in this region. However, it is clearly seen from Fig. 5(a) that a non-negligible intensity contribution, represented in black on the image, appears just at the injector exit. This detected light, which describes the general conical structure of the spray, corresponds principally to multiply scattered photons. When using structured illumination, see Fig. 5(b), this contribution is significantly suppressed highlighting both the presence and absence of liquid structures.

The light intensity profile integrated along the vertical axis of the magnified area (situated here between 5.5 mm to 10.5 mm below the nozzle tip) is provided in Fig. 6(a) for both $I_C$ and $I_S$. The signal difference $\Delta I$ between these profiles is given in Fig. 6(b). It can be seen that the position of the maximum $\Delta I$ peak coincides with the position of the maximum light intensity detected in Fig. 6(a), as indicated by the dashed lines. This intensity peak corresponds to a spray region where the secondary break-up occurs and where the number density of droplets is high. This high concentration of droplets is responsible for both the strong light intensity and the large contribution from multiple scattering. Furthermore, it can be seen that the amount of light removed from the conventional image changes significantly with position. This observation confirms the presence of strong inhomogeneities within the spray and demonstrates the capability to correct effects from *secondary emission*.

#100992 - $15.00 USD Received 2 Sep 2008; revised 9 Oct 2008; accepted 15 Oct 2008; published 20 Oct 2008

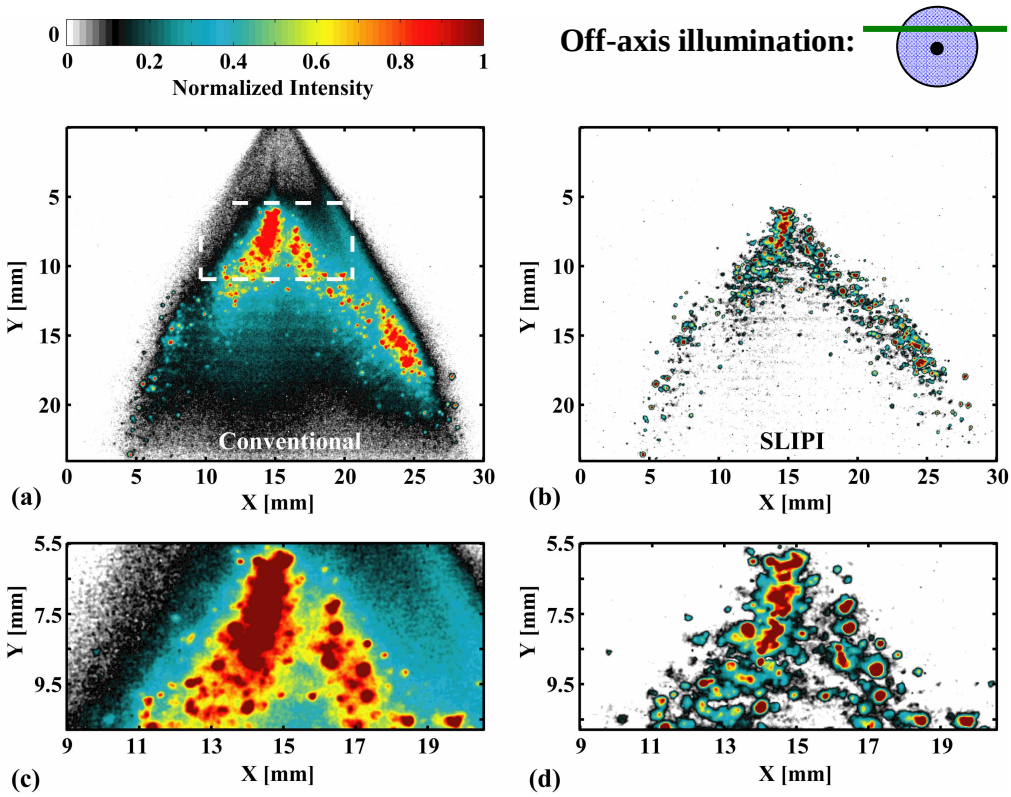


Fig. 5. Comparison between the conventional planar Mie imaging and SLIPI. The planar illumination is ~5mm off-axis (behind) from the nozzle centre. Each image corresponds to an average of 50 triple images. A magnified area indicated by the dashed lines in (a) is illustrated for the conventional and the SLIPI image in (c) and (d) respectively.

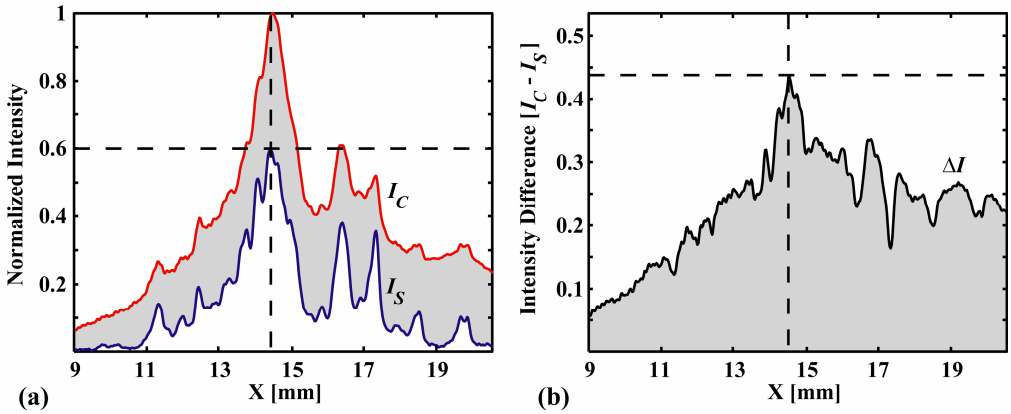


Fig. 6. Intensity profiles integrated along the vertical axis of the magnified areas given in Fig.5 (c) and (d). The light intensity difference between the conventional signal $I_C$ and the SLIPI signal $I_S$ is given in (b). The grey area indicates the contribution from multiple scattering removed by means of SLIPI, showing a maximum value reaching $\Delta I$ = 44%.

#100992 - $15.00 USD Received 2 Sep 2008; revised 9 Oct 2008; accepted 15 Oct 2008; published 20 Oct 2008

*4.2 Application to a nebulizer*

As mentioned previously, the total time needed to record the three images for the setup presented here was larger than 110 $\mu$s. At this time separation, no pixel-to-pixel displacement between the first and the last image occurs for flow velocity below a maximum of 25 cm/s. This velocity limit is not adequate for the acquisition of a "single shot" SLIPI image within the hollow-cone spray, where the velocity of the droplets reaches 50 m/s [20]. However, by imaging a sufficiently slow flow motion, liquid structures can be frozen in time within a single "triple image" scenario. In this section we investigate a dilute flow of small water droplets (below 5 $\mu$m in diameter) created by a nebulizer. A stream of nitrogen is introduced in the center of the nebulizer creating an inner region. Despite the fact that no droplets are present within the nitrogen stream, the intensity measured from this region is non-zero in the conventional image (see Fig. 7(a) and (c)). Furthermore, the conventional image shows large continuous structures which do not provide a correct illustration of the droplet flow. When using structured illumination the unwanted light intensity is suppressed, highlighting structure separations and voids in the image (see Fig. 7(b) and (d)). The resultant SLIPI image reveals a more realistic structure of the nebulizer where droplets are already well formed and separated in space. These results, which are analyzed in detail by Kristensson *et al.* [20], demonstrate the capability of SLIPI to capture a dynamic flow.

The investigation of faster flow motion requires the time delay from shot-to-shot to be decreased. One approach is to use a thicker rotating glass plate. Another solution is to use a grating with a higher spatial frequency. However, it should be noted that the use of finer grids lead ultimately to a decrease of the modulation depth which will affect the effectiveness of the technique.

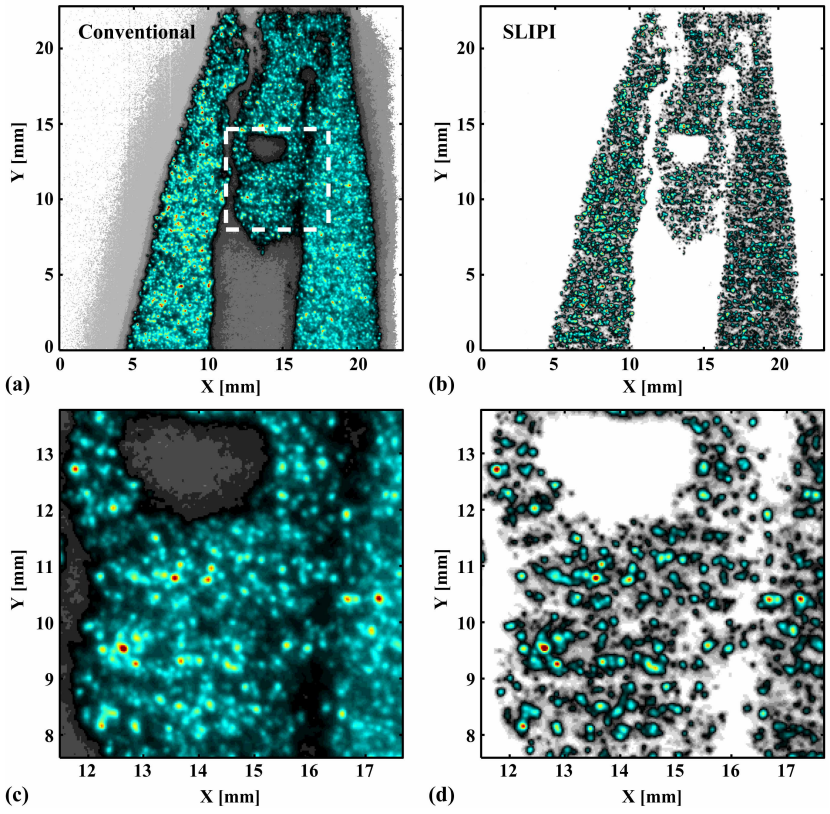


Fig. 7. Comparison between conventional planar Mie imaging in (a) and (c) and SLIPI in (b) and (d) for a "single shot" triple image (see Kristensson *et al.* [20] for more details).

#100992 - $15.00 USD Received 2 Sep 2008; revised 9 Oct 2008; accepted 15 Oct 2008; published 20 Oct 2008

Finally, by using three gratings (instead of one) along each beam path, the rotating glass plate could be removed. In this case, the minimum time separation will instead be only governed by the camera or the laser system. Note that the optimization of the technique will be further investigated.

## 5. Conclusion

In summation, we have demonstrated the capability of a novel technique for the suppression of the multiple light scattering in laser sheet images of a spray operating in the atomization regime. The technique was tested on a typical hollow-cone water spray based on the Mie scattering detection. It has been quantitatively measured that 44% of light intensity, arising from *secondary emission*, could be removed in a region where secondary break-ups were occurring. Furthermore, an increase in image contrast from 55% to 80% could be achieved in the dense region of the spray. Such an improvement allows more accurate analysis and interpretation of the spray interior and structure. It has been shown that the method is suitable for averaged images, but can also be applied to "single shot" imaging. Finally, the technique enables a more accurate accounting of the effects from *laser light extinction* and can promisingly be implemented to other planar laser diagnostics, such as Planar Liquid Laser Induced Fluorescence and simultaneous Mie / LIF measurements.

## Acknowledgments

The authors wish to show their appreciation to the Linné Centre within the Lund Laser Centre (LLC) as well as the Centre for Combustion Science and Technology (CECOST) through SSF and STEM for financial support. The authors would like to acknowledge also Dr. Ulf Göransson and Dr. Bjarne Paulsen Husted for lending their spray equipment.

#100992 - $15.00 USD Received 2 Sep 2008; revised 9 Oct 2008; accepted 15 Oct 2008; published 20 Oct 2008